

## DESIGN OF A $MgB_2$ BEAM TRANSPORT CHANNEL FOR A STRONG-FOCUSING CYCLOTRON\*

K. Melconian, C. Collins, K. Damborsky, J. Kellams, P. McIntyre, N. Pogue, A. Sattarov  
Accelerator Research Laboratory, Department of Physics and Astronomy, Texas A&M University,  
TX 77843, USA

### Abstract

A superconducting strong focusing cyclotron is being developed for high current applications. Alternating-gradient focusing is provided by  $\sim 6$  T/m superconducting beam transport channels which lie in the sectors along the arced beam trajectory of each orbit of the cyclotron. The  $\sim 1$  T sector dipoles, corrector dipoles, and Panofsky type quadrupoles utilize  $MgB_2$  superconductor operating around 15-20 K. The operating temperature provides a valuable margin for a cost-effective cryogenic design, and large thermal stability in the event of occasional heat loads from intercepted beam or other sources. The main dipole windings are designed with sufficiently large curvature so that they can be fabricated using react-and-wind procedure; the quadrupole windings require small-radius end bends and so must be fabricated using wind-and-react procedure. Initial magnetic modelling on the end field region is presented. This paper is a duplicate of work previously presented [1].

### INTRODUCTION

High-current proton accelerators are being developed for use as neutron and muon sources, accelerator driven systems (ADS) for nuclear transmutation, high energy physics and nuclear physics research experiments, cancer therapy, and isotope production. The Accelerator Research Lab at Texas A&M University (TAMU) is developing an accelerator-driven subcritical molten salt system to destroy the transuranics in spent nuclear fuel. Details of the ADS can be found in references [2] and [3]. The proton driver for the system is a flux-coupled stack of 10 mA 800 MeV CW strong-focusing cyclotrons (SFC) which incorporate several novel techniques to provide low-loss acceleration of such high-current beams.

There are a number of challenges in accelerating high current beams in a cyclotron: including crossing betatron tune resonances, space charge effects, and sufficient turn separation at high energies. These challenges are addressed in the SFC through several innovations: novel superconducting RF cavities [4] combined with a low dipole field make it possible to fully separate the orbits; multiple cyclotrons can be stacked in a flux-coupled arrangement to provide reliability by redundancy; and strong-focusing is accomplished using alternating-gradient beam transport channels (BTC) located in the aperture of the sector dipoles.

### SECTOR DIPOLE

The SFC accelerator system, shown in Fig. 1, consists of an injector cyclotron (TAMU100) and a main cyclotron (TAMU800). Each cyclotron is an isochronous continuous-wave (CW) sector cyclotron containing wedge-shaped sector dipoles and superconducting RF cavities. The flux-coupled stacked configuration of the cyclotrons was chosen to minimize the overall footprint, provide the required current for our accelerator-driven molten salt system, and provide reliability by redundancy.

The sector dipole is designed using the levitated-pole strategy first developed for the RIKEN ring cyclotron [5]. The main dipole field is provided by  $MgB_2$  superconducting windings around a pair of cold-iron flux plates. Each assembly of two flux plates is suspended symmetrically in the vacuum gap of the overall warm-iron flux return. The back-side gaps between each flux plate and its warm-iron flux return segment is designed so that net vertical forces on each cold-iron flux plate cancels. This means the thermally insulating supports for each flux plate need only support the gravitational force plus modest de-centering forces. The fields along the design orbits required for isochronicity are obtained by shaping the beam side of the cold pole pieces. A list of some of key parameters of the TAMU 100 and TAMU 800 are given in Table 1.

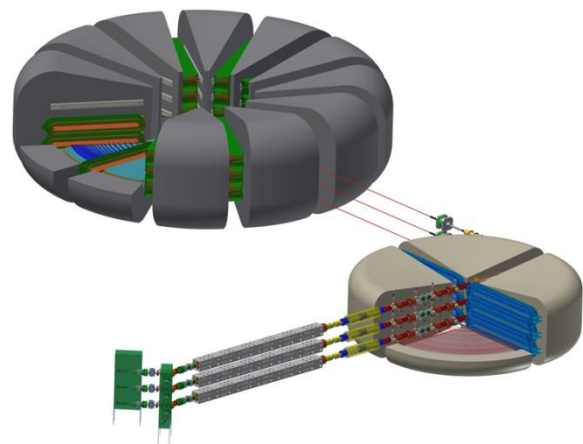


Figure 1: Sequence of strong-focusing cyclotrons consisting of two stacked cyclotron systems. The TAMU 100 accelerates protons from the RFQ to 100 MeV and feeds into the TAMU 800 which accelerates the protons to a final energy of 800 MeV.

\*Work supported by Texas ASE Fund and by the Mitchell Family Foundation.

# KarieMelconian@tamu.edu

Table 1: Cyclotron Parameters of the TAMU 100 and TAMU 800

Parameter	TAMU 100	TAMU 800
Injection E	6.5 MeV	100 MeV
Extraction E	100 MeV	800 MeV
B	0.3-0.5 T	~1 T
Dipole aperture	7 cm	7 cm
Sector angle	90	30
# of sectors	4	12
# of RF cavities	2	10

### BEAM TRANSPORT CHANNEL

An array of beam transport channels is installed in the aperture between flux plates. The spiral pattern of BTCs defines the equilibrium orbit of the cyclotron. Each arch-shaped channel spans half the width of the sector dipole, as shown in Fig. 2. Each BTC contains a single-layer wire-wound quadrupole winding and a trim dipole winding, as shown in the close-up in Fig. 3.

The quadrupole winding on each channel is configured as two successive windings that provide a complete F-D alternating-gradient cell in each sector dipole.

The trim dipole winding is the outermost layers on the left and right sides of the channel shown in Fig. 3. It is used to maintain isochronicity, and to open the orbit spacing at injection and extraction for which it serves as a built-in septum. The strength of dipole trim winding is ~2% of the main dipole field, or about 20 mT. The trim dipoles on the first and last channels will be wound with multiple layers to provide a more robust septum function.

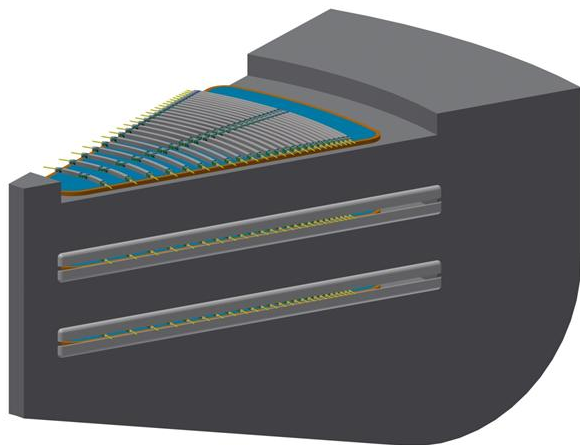


Figure 2: One of the TAMU800 sectors with the top flux return removed to show the arrangement of beam transport channels on the cold pole piece. BTCs are arranged as FD pairs to provide focusing.

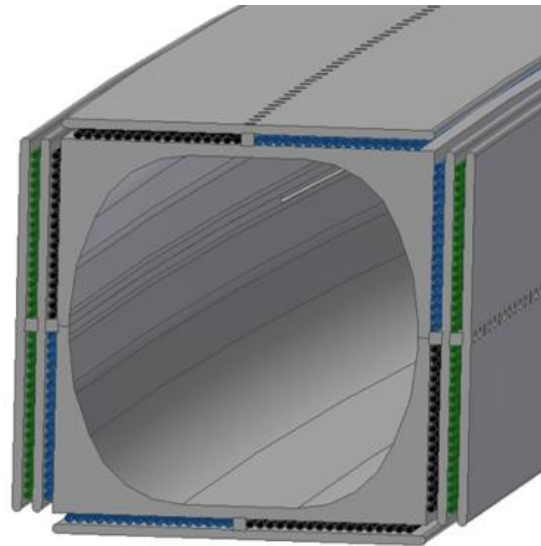


Figure 3: The image shows a cross section of the planned winding. The inner windings (blue and black) produce the quadrupole and the outer trim dipole (green) winding is located on the sides.

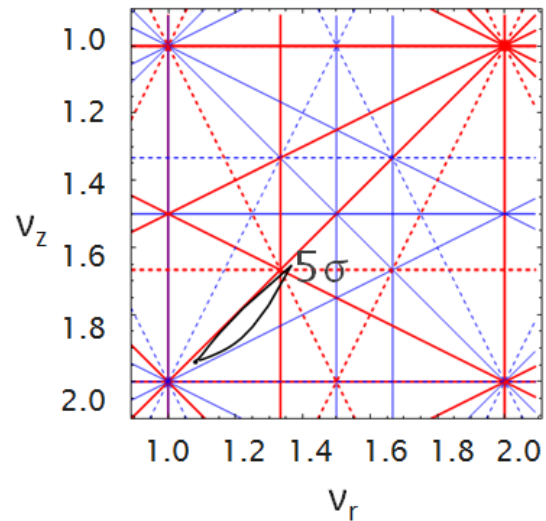


Figure 4: Tune plot for a 10 mA beam from injection to extraction in the TAMU 100 showing the tune can be fully controlled. The tail of the tune footprint is  $5\sigma$ .

### Optics

A common design challenge for cyclotrons is to try to limit resonance crossings which can lead to beam blow-up. The SFC makes it possible to lock the betatron tunes to a single favourable value for all energies from injection to extraction as illustrated in Fig. 4. This is the typical operation for a synchrotron or linac, but has never before been possible in a cyclotron because conventional cyclotrons rely upon fringe-field focusing at sector edges for their tunes, particles are free to deviate from the ideal helical reference orbit by any field error, timing error, or deviation from ideal cavity phase and amplitude.

Two cases were considered for the arrangement of focusing (F) and defocusing (D) quadrupoles along each dipole sector, the doublet FD and the triplet FDF. For the TAMU 100, the triplet arrangement was found to provide more control of the tune, while a doublet was sufficient for the TAMU 800. The layout of the two BTC on the cold pole piece of the sector magnet can be seen in Fig. 2.

### Modelling

We have chosen a 5 cm square Panofsky-style quadrupole [6], which differs somewhat from a traditional Panofsky quadrupole in that it has unsaturated iron boundaries only on the top/bottom faces. In a traditional Panofsky quadrupole, the current distribution required for an ideal quadrupole is uniform across the square or rectangular aperture. For our case, we compensate for the effect of the side vacuum boundaries by adjusting the wire configuration in the current sheet, so as to produce a substantially pure quadrupole field in the interior of the channel. Magnetic modeling was performed using the finite element computer code Comsol [7].

For the main body of the BTC, a 2D cross-section was used with iron slabs above and below. The model assumed a 1.15 mm diameter wire, 1 mm for the wire and an additional 0.15 mm for the s-glass insulation. The model also included a 1T external field to ensure a proper magnetic response from the iron and to provide an estimate of the maximum magnetic field the superconducting wire will experience. The higher-order multipoles are calculated with a reference radius of 70% of the beam tube. Using this 2D model, the current density to achieve 6 T/m was found to be  $\sim 2.3 \times 10^4$  A/cm<sup>2</sup>.

The 3D modeling of the end-cap has not yet been done on an individual wire scale. Instead, the wires were treated as a rectangular package and swept around the end-cap as shown in Fig. 5. As with the 2D model, the multipoles were calculated with a reference radius of 70% of the beam aperture at 2 mm steps starting from the main body out along the beam path to 80 mm. A plot of the multipoles along the end-cap and the total integrated multipoles are shown in Fig. 6 and Fig. 7, respectively.

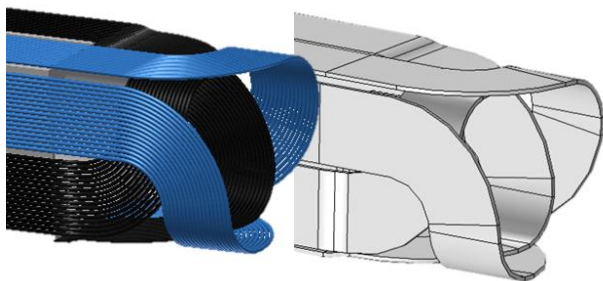


Figure 5: Actual quadrupole wire paths are shown on the left and the rectangular package used to represent the wires for modelling are shown on the right.

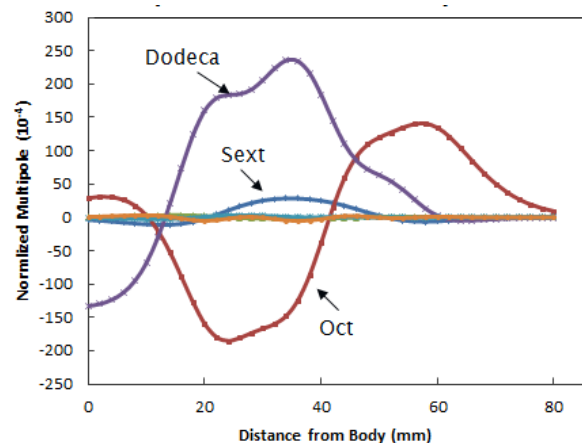


Figure 6: Multipole normalized to the body quadrupole starting at the main body of the magnet out to 80 mm. Only the largest multipoles are labelled.

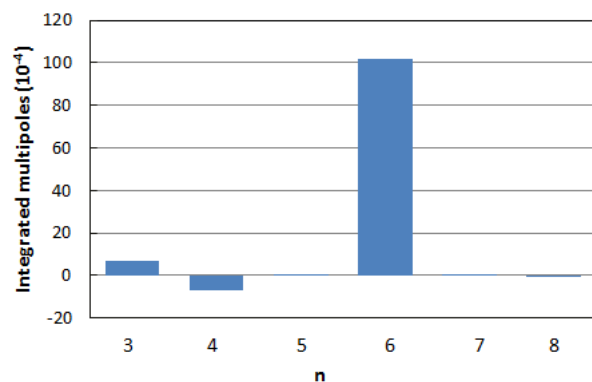


Figure 7: The integrated multipoles for one end cap normalized to the quadrupole strength in the body of the beam transport channel. Here  $n=3$  refers to the sextupole term,  $n=4$  octupole, etc.

### Mechanical Design

Many of the physical parameters of the quadrupole are defined by the optics and geometry of the main dipole magnets. The 7 cm spacing between each pair of cold-iron flux plates of the dipole must house the superconducting BTCs and the cryogenic cooling for the channels, but also maintain the maximum possible fraction of aperture clear for the high-current beam. The minimum beam separation at extraction produced by the superconducting RF cavities and moderate dipole field is 5.6 cm, which further restricts the dimension of the BTC.

Our choice of MgB<sub>2</sub> places two more restrictions on the design. The first is the green state strain sensitivity of the wire which requires we maximize our minimum bend radius. In order to produce the largest bend, the wires must turn around on the end-cap in the manner shown in Fig. 8. This complicates the end-cap winding into a series of nested layers. The second issue in using wind-and-react MgB<sub>2</sub> is the material used in the winding must be able to withstand the 650-700°C heat treatment. This prevents us from using a direct wind approach.

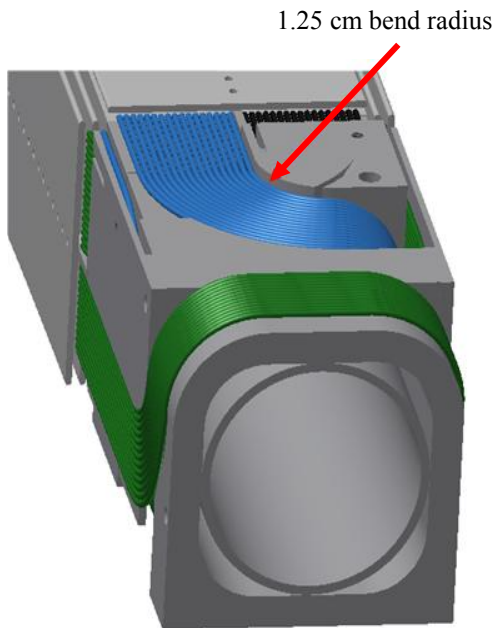


Figure 8: End-cap region showing the minimum bend radius for the second layer (blue) of quadrupole winding. The dipole is the outermost winding (green).

The curve of the BTC poses another difficulty in winding and causes the wires to want to pull from the body on the inside arc. A set of stainless steel plates has been attached to all sides to prevent the wires from pulling off and to more easily wind the dipole layer over the quadrupole windings. The set of plates and planned winding scheme for the quadrupole and trim dipole for our prototype BTC end-cap is shown in Fig. 8.

### MgB<sub>2</sub>

From the required current density, external field, and desired operating temperature, we have chosen MgB<sub>2</sub> for the superconducting wire in the BTCs. For similar reasons, MgB<sub>2</sub> was chosen for the windings of the main dipoles, allowing both the BTC and dipole cold pieces to operate at the same temperature. The sector dipoles and the beam transport channels within constitute the first systems that will intercept protons lost from a bunch. Due to the heat load expected from proton impacts, the thermal stability of the superconducting material is of critical importance in the BTC and sector dipole designs. With the requisite current densities and peak field listed in Table II, MgB<sub>2</sub> wires can operate in a temperature range of 15–20 K [8]. The thermal margin at 15 K for the 6 T/m gradient is ~3 K and increases to ~9 K for the 2 T/m case [9]. Additionally, this operating temperature range has the dual benefits of decreasing refrigeration cost by ~10x compared to LTS materials while subsequently increasing the heat capacity of the conductor and structural materials alike, providing a stabilization against short term beam losses.

The small bending radius required for the channel windings would produce a strain,  $\epsilon$ , larger than the irreversible strain degradation limit (0.3-0.4%) allowed for react-and-wind MgB<sub>2</sub>, so a wind-and-react method must be used. While the irreversible strain limits of react and wind MgB<sub>2</sub> have been well studied [10], the sensitivity of green state (unreacted) to pre-reaction strain is less understood. Anecdotal evidence has previously established that  $\epsilon > 6\%$  has led to irreversible degradation of Ic in superconducting wires [9]. Discussions with our wire vendor, Hypertech [11], and space limitations imposed from our geometry, led to a winding scheme that maximized our minimum bend radius resulting in a 1.25 cm minimum bend radius for the BTC windings. Previous studies on wind-and-react MgB<sub>2</sub> wires have shown that a strain over 6% lead to significant current degradation, while staying under 2% had little to no degradation. Our bend radius corresponds to a 3.8% max strain, which is in an unexplored area for current degradation from bending strain. We have performed initial studies which indicate a strain up to 5% may be tolerated without appreciable loss of transport properties [12]. Table 2 lists some of the important parameters of the beam transport channel and MgB<sub>2</sub> wire. Coils will be cooled using cold He vapor to maintain the 15-20 K operating temperature.

Table 2: Beam Transport Channel Parameters

Quadrupole gradient	2-6 T/m
Trim dipole	~20 mT
Operating temperature	15-20 K
Min. bend radius	1.25 cm
Peak coil field	1.4 T
Current density	$2.4 \times 10^4$ A/cm <sup>2</sup>
Wire diameter	1 mm

## CONCLUSION

A strong-focusing cyclotron is being developed capable of accelerating 10 mA CW proton beams to 800 MeV for use in an accelerator-driven molten salt system or for other high-power cyclotron applications. Magnetic modeling of the sector dipole and beam transport channels show MgB<sub>2</sub> to be a viable candidate for the superconducting windings. A winding strategy has been developed which limits the minimum bend radius strain on the wire to 3.8%. Previous studies have shown little to no degradation up to 5%. Initial modeling on the higher order multipoles has also been performed.



## ACKNOWLEDGMENT

This work has been supported by grants from the Texas ASE Fund and by the Mitchell Family Foundation. The authors would also like to thank Mike Tomsic of HyperTech; Mike Sumption of OSU; Saeed Assadi, Alfred McInturff, Tim Elliot, and Andrew Jaisle from the Accelerator Research Laboratory at Texas A&M University; and John Buttles of Bailey Tool and Manufacturing for prototype manufacturing and design discussions.

## REFERENCES

- [1] K. Melconian, C. Collins, K. Damborsky, J. Kellams, P. McIntyre, N. Pogue, and A. Sattarov, "Design of A MgB<sub>2</sub> Beam Transport Channel for a Strong-Focusing Cyclotron," *IEEE Transaction on Applied Superconductivity* (2013).
- [2] E. Sooby, A. Baty, O. Benes, P. McIntyre, N. Pogue, M. Salanne, and A. Sattarov, "Candidate Molten Salt Investigation for an Accelerator Driven Subcritical Core," *J. Nucl. Mater.*, Vol. 440 (2013).
- [3] S. Assadi, K. Badgley, J. Kellams, N. Pogue, and A. Sattarov, "Strong-focusing Cyclotron for High-current Applications," in *IPAC*, New Orleans (2012).
- [4] N. Pogue, P. McIntyre, and A. Sattarov, "Superconducting RF Cavity for High-current Cyclotrons," presented at the IPAC New Orleans, LA, USA (2012).
- [5] T. Kawaguchi, T. Kubo, T. Mitsumoto, H. Okuno, T. Tominaka, J.W. Kim, S. Fujishima, K. Ikegami, N. Sakamoto, S. Yokouchi, T. Morikawa, Y. Tanaka, A. Goto, and Y. Yano, "Design of the Sector Magnets for the RIKEN Superconducting Ring Cyclotron," *Proceedings of the 1997 Particle Accelerator Conference*, Vols. 1-3 (1998) 3419-3421.
- [6] L.N. Hand and W.K.H. Panofsky, "Magnetic Quadrupole with Rectangular Aperture," *Review of Scientific Instruments*, Vol. 30 (1959) 927-930.
- [7] COMSOL. Available: <http://www.comsol.com/>
- [8] S.L. Bud'ko, G. Lapertot, C. Petrovic, C.E. Cunningham, N. Anderson, and P.C. Canfield, "Boron Isotope Effect in Superconducting MgB<sub>2</sub>," *Phys. Rev. Lett.*, Vol. 86 (Feb. 26, 2001) 1877-1880.
- [9] G.Z. Li, Y. Yang, M.A. Susner, M.D. Sumption, and E.W. Collings, "Critical Current Densities and n-Values of MgB<sub>2</sub> Strands over a Wide Range of Temperatures and Fields," *Superconductor Science & Technology*, Vol. 25 (February 2012).
- [10] M.D. Sumption, S. Bohnenstiehl, F. Buta, M. Majoros, S. Kawabata, M. Tomsic, M. Rindfleisch, J. Phillips, J. Yue, and E.W. Collings, "Wind and React and React and Wind MgB<sub>2</sub> Solenoid, Race Track and Pancake Coils," *IEEE Transactions on Applied Superconductivity*, Vol. 17 (June 2007) 2286-2290.
- [11] HyperTech. Available: <http://www.hypertechresearch.com>
- [12] K. Melconian, K. Damborsky, N. Glasser, E. Holik, J. Kellams, P. McIntyre, N. Pogue, and A. Sattarov, "Design and Development of a MgB<sub>2</sub>-based Sector Dipole and Beam Transport Channel for a Strong-Focusing Cyclotron," in *CEC/ICMC*, Anchorage, AK (2013).